# On the use of symmetrizing variables for vacuums

Thierry Gallouët, Jean-Marc Hérard, Nicolas Seguin

# On the use of some symmetrizing variables to deal with vacuum

Thierry Gallouët[1] , Jean-Marc Hérard[1,2] , Nicolas Seguin[1]

[1] Université de Provence, Centre de Mathématiques et d'Informatique,
Laboratoire d'Analyse, Topologie et Probabilités - UMR CNRS 6632,
39 rue Joliot Curie, 13453 Marseille cedex 13, FRANCE
gallouet@cmi.univ-mrs.fr Tel: 04-91 11 35 42

[2] Électricité de France, Division Recherche et Développement,
Département Mécanique des Fluides et Transferts Thermiques,
6 quai Watier, 78401 Chatou cedex, FRANCE
herard@cmi.univ-mrs.fr - herard@chi80bk.der.edf.fr
seguin@chi80bk.der.edf.fr Tel: 1- 30 87 70 37

**Abstract**

The paper is devoted to the computation of shallow-water equations (or Euler equations) when using some approximate Godunov scheme called VFRoe, when the flow may include dry areas (or very low density regions). This is achieved with help of some symmetrizing variables. The whole enables to insure the discrete preservation of positive variables on interfaces, and meanwhile to compute vacuum occurence or propagation of shock waves over near-vacuum. A short section is also dedicated to the non conservative hyperbolic equations arising within the frame of one-equation or two-equation turbulent compressible models. Many numerical tests confirm the capabilities of the scheme, and measure of $L^1$ error norm in some particular cases enables to detail the actual rate of convergence.

*Keywords:* finite volume scheme, approximate Godunov scheme, Riemann problem, positive variables, symmetrizing variables.

An abridged version of the paper has been presented during the 15th AIAA CFD Conference (AIAA paper 2001-2670)

# 1 Introduction

The paper examines the suitability of some approximate Godunov schemes to deal with computation of either shallow water equations or Euler equations (including turbulence model or not) when vacuum occurs in the solution. This may happen in the latter frame when strong double rarefaction waves propagate, or when some shock wave expands over a dry area. In the former frame, it is well known that the use of the exact Godunov scheme [1], or other approximate Riemann solvers hardly provides satisfactory results when bluff bodies are present in the computational domain [2, 3, 4, 5, 6], or when computing flows in safety valves for instance. Thus, we propose herein an alternative *numerical* way to deal with vacuum in each case, based on the use of an approximate Godunov scheme combined with a particular choice of symetrizing variables. The method aims at providing suitable interface values of states, and we emphasize that it does not imply that cell values of states are physically admissible due to the averaging procedure, which is not a projection method (unlike when using the exact Godunov scheme).

Vacuum may of course occur rigorously when focusing on shallow water equations, since the water height may either become null when flow is leaving some area, which is usually connected with presence of variations in topography, or may be a relevant initial condition, for instance when simulating some dam breakdown. We emphasize that the suitability of the Euler equations to provide correct description of the flow including low density regions (or near vacuum) is not a silly assumption, and that it can hardly be replaced by simulation of Boltzmann equations, in many circomstances, unless the main part of the physics investigated is disregarded. Thus current problems should not be confused with those where the rarefied gas approach should be prefered (in that case, some schemes such as the DSMC method may of course be privileged, and the reader is referred to reviews pertaining to that field [7], [8]). The problem of the coupling of Euler equations with Boltzmann equations, which seems indeed a promising way for improvment of local prediction of flows, is also beyond the scope of the present work, and cannot be imposed in many industial situations, since vacuum only arises in some specific cases, at a certain time in the simulation, in the close vicinity of particular regions. The problem of the capability of current computer facilities to cope with any range of -high- Knudsen number must also be accounted for, and the accuracy of the model should not be confused with the accuracy of numerical methods involved in computations. We also eventually underline that the problem of vacuum becomes even more crucial when trying to compute some particular unsteady cases arising in the frame of two phase flows, especially when focusing on fluid flows in nuclear power plants. For instance, the problem of predicting flashing flows in safety valves (which may require to use Euler equations with complex EOS or alternatively the Homogeneous Relaxation Model) filled with pressurised water is a good challenge for people working in the numerical community, since both high density and low density regions are present in the field.

A first section is dedicated to the general presentation of the approximate Godunov scheme nicknamed VFRoe [9, 10, 11] when applying for non conservative variables. It requires solving a linearised Riemann problem at each interface in order to evaluate an approximate interface state; the numerical flux is then defined by computing the exact flux function for given approximate interface state. This formalism should not be confused with Godunov-type schemes, which have been introduced in [12] and require consistency with the integral form of the conservation law and consistency with the entropy inequality. A first version of the former scheme has been used to investigate a rather wide variety of industrial applications computing Euler equations with help of variable $(1/\rho, u, p)$. The main idea in this paper concerns the use of some symmetrizing variables to determine an approximate interface state by linearizing the symmetric form of the system. We

recall that the symmetrised form of first order set of PDE is as follows:

$$M(Y)\frac{\partial Y}{\partial t} + B(Y)\frac{\partial Y}{\partial x} = 0 \tag{1}$$

where $Y$ is the symmetrizing variable, and $M(Y)$ (and $B(Y)$) respectively stands for some symmetric positive definite matrix (respectively symmetric matrix). We also recall that using the latter variables enables to prove theoretical existence of a linearisation in the sense of Roe [13], which is strongly linked with the existence of an entropy function for hyperbolic systems under conservative form. Nevertheless, they are seldomly used in numerical methods in practice except perhaps when building Petrov-Galerkine weak formulations using the Finite Element Method (see for instance [14]). We emphasize that the technique presented here is devoted to Finite Volume approximations, and the suitability of the choice of symetrizing variables will be discussed.

Afterwards, the framework of shallow water equations is briefly examined when restricting to symmetrizing variables [10] $(u, 2c)$. It will be shown that numerical vacuum appears at the interface exactly when real vacuum occurs in the continuous solution. The specific case [15, 16] where bottom slopes should be accounted for (which results in the fact that the whole system is no longer under conservative form) is discussed in detail in a companion paper [17]. The third section is devoted to the Euler equations with arbitrary equation of state, though practical numerical examples focus on perfect gas Equation of State (EOS). More emphasis is given on this section, and focus is given on variable $(s, u, p)$. It will be seen that a condition -which is slightly more restrictive than the one dedicated to exact vacuum occurence- enables to insure positivity of interface values of density and pressure. A short section completes the paper by focusing on the convective part of a four equation model arising when computing compressible K-epsilon models. In this case too, numerical vacuum may occur in the solution at the interface before it occurs in the exact solution of the Riemann problem, but a scalar condition - which is not much constraining- enables to insure positive values of mean density, mean pressure and turbulent kinetic energy at the interface.

Actually, there is a great similarity in all "Euler-type" systems discussed herein. The three of them require that one scalar condition on initial data holds ((14) for Euler equations for instance), otherwise vacuum occurs in the exact solution. Considering then the problem of approximating solutions of the latter, it clearly appears that all approximate Riemann solvers usually involve intermediate states which :
(i) do not satisfy preservation of Riemann invariants through the contact discontinuity -if any-,
(ii) require that $k_0$ distinct scalar conditions should be fulfilled in order to insure that $k_0$ (expected) positive components are non-negative.
The proposed strategy aims at providing some remedy to that failure.

This approach also concerns workers in the field of statistical description of turbulence, using full Reynolds stress closures and Favre averaging process.

## 2 Basic principle of VFRoe schemes

We briefly recall herein the basis of VFRoe scheme with non conservative variables. We restrict for the sake of simplicity to regular meshes of size $\Delta x$ such that: $\Delta x = x_{i+\frac{1}{2}} - x_{i-\frac{1}{2}}$, $i \in \mathbb{Z}$, and denote as usual $\Delta t$ the time step, where $\Delta t = t^{n+1} - t^n$, $n \in \mathbb{N}$.
We define $W \in \mathbb{R}^p$ the exact solution of the non degenerated hyperbolic system:

$$\left\{ \begin{array}{l} \dfrac{\partial W}{\partial t} + \dfrac{\partial F(W)}{\partial x} = 0 \\ W(x,0) = W_0(x) \end{array} \right.$$

with $F(W)$ in $\mathbb{R}^p$. Let $W_i^n$ be the approximate value of $\frac{1}{\Delta x}\int_{x_{i-\frac{1}{2}}}^{x_{i+\frac{1}{2}}} W(x,t^n)dx$. Integrating over $[x_{i-\frac{1}{2}};x_{i+\frac{1}{2}}]\times[t^n;t^{n+1}]$ provides:

$$W_i^{n+1} = W_i^n - \frac{\Delta t}{\Delta x}\left(\phi_{i+\frac{1}{2}}^n - \phi_{i-\frac{1}{2}}^n\right)$$

where $\phi_{i+\frac{1}{2}}^n$ stands for the numerical flux through the interface $\{x_{i+\frac{1}{2}}\}\times[t^n;t^{n+1}]$. The time step is in agreement with some CFL condition in order to gain stability. Thus $\phi_{i+\frac{1}{2}}^n$ only depends on $W_i^n$ and $W_{i+1}^n$ when restricting to first order schemes. Whatever the scheme is, the numerical flux complies with consistent condition (see [4]):

$$\phi(V,V) = F(V)$$

We present now approximate Godunov fluxes $\phi(W_L,W_R)$ associated with the 1D Riemann problem:

$$\left\{\begin{array}{l} \dfrac{\partial W}{\partial t} + \dfrac{\partial F(W)}{\partial x} = 0 \\ W(x,0) = \left\{\begin{array}{ll} W_L & \text{if } x<0 \\ W_R & \text{otherwise}\end{array}\right. \end{array}\right. \tag{2}$$

and initial condition: $W_L = W_i$ and $W_R = W_{i+1}$, $i\in\mathbb{Z}$.

VFRoe scheme is an approximate Godunov scheme where the approximate value at the interface between two cells is computed as detailed below. Let us consider some change of variable $Y = Y(W)$ in such a way that $W_{,Y}(Y)$ is invertible. The counterpart of above system for regular solutions is:

$$\frac{\partial Y}{\partial t} + B(Y)\frac{\partial Y}{\partial x} = 0$$

where $B(Y) = (W_{,Y}(Y))^{-1}A(W(Y))\ W_{,Y}(Y)$ ($A(W)$ stands for the Jacobian matrix of flux $F(W)$).

Now, the numerical flux $\phi(W_L,W_R)$ is obtained by solving the linearized hyperbolic system:

$$\left\{\begin{array}{l} \dfrac{\partial Y}{\partial t} + B(\hat{Y})\dfrac{\partial Y}{\partial x} = 0 \\ Y(x,0) = \left\{\begin{array}{ll} Y_L = Y(W_L) & \text{if } x<0 \\ Y_R = Y(W_R) & \text{otherwise}\end{array}\right. \end{array}\right. \tag{3}$$

where $\hat{Y}$ agrees with the condition: $\hat{Y}(Y_L,Y_L) = Y_L$, and also $\hat{Y}(Y_L,Y_R) = \hat{Y}(Y_R,Y_L)$.

Once the exact solution $Y^*(\frac{x}{t};Y_L,Y_R)$ of this approximate problem is obtained, the numerical flux is defined as:

$$\phi(W_L,W_R) = F(W(Y^*(0;Y_L,Y_R)))$$

Let us set $\widetilde{l_k}$, $\widetilde{\lambda_k}$ and $\widetilde{r_k}$, $k=1,...,p$, left eigenvectors, eigenvalues and right eigenvectors of matrix $B(\overline{Y})$ respectively. The solution $Y^*(\frac{x}{t};Y_L,Y_R)$ of the linear Riemann problem is defined everywhere (except along $\frac{x}{t} = \widetilde{\lambda_k}$):

$$\begin{aligned} Y^*\left(\frac{x}{t};Y_L,Y_R\right) &= Y_L + \sum_{\frac{x}{t}>\widetilde{\lambda_k}} ({}^t\widetilde{l_k}.(Y_R-Y_L))\widetilde{r_k} \\ &= Y_R - \sum_{\frac{x}{t}<\widetilde{\lambda_k}} ({}^t\widetilde{l_k}.(Y_R-Y_L))\widetilde{r_k} \end{aligned}$$

Combining the last equalities enables to write the latter in a slightly different form:

$$Y_R - Y_L = \sum_{k=1,p} ({}^t\widetilde{l_k}.(Y_R - Y_L))\widetilde{r_k} = \sum_{k=1,p} \tilde{\alpha}_k \widetilde{r_k} \tag{4}$$

setting: $\tilde{\alpha}_k = {}^t\widetilde{l_k}.(Y_R - Y_L)$.

Before going on, we recall that the Basic VFRoe scheme was first proposed in [18], and was based on the choice $Y(W) = W$ and thus $B(\overline{Y}) = A(\overline{W})$. (we recall that $A(W)$ is the Jacobian matrix of $F(W)$, and we note throughout the paper: $\overline{\phi}_{LR} = (\phi_L + \phi_R)/2$ whatever $\phi$ is). Other choices for Euler equations have already been examined [9],[19].

Hence, the explicit form of the Finite Volume method called VFRoe will be:

$$W_i^{n+1} - W_i^n + \frac{\Delta t}{\Delta x}\left(F(W(Y^*(0; Y_i^n, Y_{i+1}^n))) - F(W(Y^*(0; Y_{i-1}^n, Y_i^n)))\right) = 0$$

Despite from its name, it is emphasised that VFRoe scheme should not be confused with the approximate riemann solver proposed by P.L. Roe. We now examine specific schemes obtained when dealing with symmetrizing variables.

# 3 Shallow-water equations

## 3.1 Governing equations

In a one dimensional framework, shallow-water equations may be written in conservative form, using conservative variable $W = {}^t(h, hu)$, noting $h$ the water height, $u$ and $Q = hu$ the velocity and the momentum (or discharge) respectively, and $g$ the gravity constant:

$$h_{,t} + (hu)_{,x} = 0 \tag{5a}$$

$$(hu)_{,t} + \left(hu^2 + g\frac{h^2}{2}\right)_{,x} = 0 \tag{5b}$$

Vacuum will occur when both momentum and water height vanish: $h = hu = 0$. Note that in this case $u$ is undefined. Otherwise the solution of the associated Riemann problem is composed of three distinct states separated by two Genuinely Non Linear fields. The speed of the two waves are $u - c$ and $u + c$ respectively, noting as usual $c = \sqrt{gh}$. The intermediate state is indexed by subscript 1. Noting $h_1 = \frac{(c_1)^2}{g}$, and $Q_1 = h_1 u_1$, the standard solution of the 1D Riemann problem consists in three distinct states with subscripts L, 1 and R separated by rarefaction waves or shock waves as recalled by the following figure 1.

The one dimensional Riemann problem has a unique entropy consistent solution with no vacuum occurence provided that initial data satisfies the following condition:

$$u_R - u_L < 2(\sqrt{gh_R} + \sqrt{gh_L}) \tag{6}$$

### 3.2 Symmetrizing variables

This system may be written in terms of non conservative variable $Y(W) = {}^t(2c, u)$ in a symmetrized form setting in (1):

$$B(Y) = \begin{pmatrix} u & c \\ c & u \end{pmatrix} \quad \text{and} \quad M(Y) = \begin{pmatrix} 1 & 0 \\ 0 & 1 \end{pmatrix}$$

Matrix $B(Y)$ is clearly symmetric and $M(Y)$ is the identity matrix which of course is symmetric positive definite.

### 3.3 Approximate Godunov scheme VFRoe using symmetrizing variable

We turn now to the associated linearised problem, and set for any quantity $\psi$: $(\Delta\psi)_{LR} = \psi_R - \psi_L$. The computation of the intermediate state in the linearised solver at each interface between two cells labelled $L, R$ is straightforward (we set here: $\hat{Y} = \overline{Y}$):

$$u_1 = \overline{u}_{LR} - (\Delta c)_{LR} \quad \text{and} \quad c_1 = \overline{c}_{LR} - \frac{(\Delta u)_{LR}}{4}$$

Note that the linearization has been made around the state $(2\overline{c},\overline{u})$. The numerical flux thus writes:

$$Q_1 = \frac{(c_1)^2 U_1}{g} \quad \text{and} \quad \left(hU^2 + g\frac{h^2}{2}\right)_1 = (c_1)^2 \frac{2(U_1)^2 + (c_1)^2}{2g}$$

### 3.4 Some properties

*Property 1:* Vacuum arises in the intermediate state of linearized Godunov solver if and only if initial data makes vacuum occur in the exact solution of the Riemann problem associated with the non linear set of equations:

$$u_R - u_L < 2(c_L + c_R) \tag{7}$$

*Proof:* Actually, when focusing on the solution of the exact Riemann problem, vacuum may only occur when initial data is such that two rarefaction waves develop. Riemann invariants are preserved in that case, hence $u + 2c$ (respectively $u - 2c$) is constant in the 1-rarefaction wave (respectively the 2-rarefaction wave) ; if subscript 1 refers to the intermediate state in the *exact* solution of the Riemann problem, then:

$$u_R - 2c_R = u_1 - 2c_1$$
$$u_L + 2c_L = u_1 + 2c_1$$

where subscripts L and R refer to values of initial data in the Riemann problem. Using some algebra enables to rewrite the latter as:

$$u_1 = \frac{u_R + u_L}{2} - (\Delta c)_{LR} \quad \text{and} \quad c_1 = \frac{c_L + c_R}{2} - \frac{(\Delta u)_{LR}}{4}.$$

One may here check that physically releavant states (with positive values of $c_1$) imply that the former condition (6) is fulfilled. More over, it can be easily seen that this couple $(u_1, c_1)$ exactly represents the intermediate state provided by the linearised approximate Godunov scheme we

focus on. This completes the proof of property 1. Thus, the present linearized solver is well suited to handle double rarefaction waves in the solution of the exact Riemann problem, at least when predicting interface values. Due to the averaging procedure, it doesn't mean anyway that cell values of water height remain positive, since the first order scheme does not construct the projection of the approximate solution. Appendix 7*a* however shows that close to a wall boundary, the cell value of water height remains positive when a very strong rarefaction wave develops (eg when $U.n \leq 0$, where $n$ denotes the unit outward normal vector at the wall boundary), assuming standard CFL condition $CFL = 0.5$.

### 3.5 Numerical results

The computational results described below correspond to a Riemann problem with the following initial data:

$$h_L = h_R = 10 \quad \text{and} \quad u_L = -u_R = -15.$$

Constant $g$ is set to 2. The CFL number is 0.49, and the regular mesh contains 5000 nodes. Figures 2 show the approximation of water height, discharge and local velocity which have been obtained using the basic first order scheme.

Recall that the basic advantage of the symmetrical case is that it provides some good idea of the behaviour of the scheme close to wall boundary conditions when applying for the mirror technique. Though the scheme is stable, we note anyway that approximate values of velocity in the near vacuum zone (eg the end of the 1-rarefaction wave or the beginning of the 2-rarefaction wave) are poorly accurate.

We give below on figures 3 some measure of the $L^1$ norm of the error, which is plotted for two cases including the shock tube case and symmetrical double rarefaction wave discussed above, and includes comparison with results obtained using the basic Godunov scheme [1]. The measured rate of convergence is close to 0.85 in both cases, which is slightly smaller than expected 1, but is in agreement with measurements provided in [9] in the frame work of Euler equations when focusing on perfect gas EOS.

The present solver has also been used successfully when computing shallow-water equations with topography [17]. The main problem in that case is that one needs in addition to account for so-called source terms associated with mean gradient of bottom elevation. This means in particular that one has to provide some discrete approximation in such a way that steady states are perfectly preserved on any mesh size. The method relies on the so-called well-balanced scheme, as first introduced by A. Y. Leroux and co authors [15], [16] previously, and takes advantage of the potentialities of the present approximate Godunov scheme. We only provide below some results associated with a rather difficult test case, which consists in emptying a reservoir containing some bump under the initial free surface, and initially at rest. The left boundary condition corresponds to some wall condition, and the right boundary condition enables to empty the computational domain. The regular mesh contains 1000 nodes, and the discretised bump profile contains 200 cells. The CFL number here was set to 0.45. The initial condition is: $h(x, t = 0) = 0.5$, and $Q(x, t = 0) = 0$. The flow around the steady state is such that no water passes over the bump.

# 4 Euler equations

## 4.1 Governing equations

Governing Euler equations may first be written in conservative form in terms of the mean density $\rho$, the mean pressure $p$, the mean velocity $u$ and the total energy $E$ as follows:

$$\frac{\partial W}{\partial t} + \frac{\partial F(W)}{\partial x} = 0 \tag{8}$$

setting:

$$W = \begin{pmatrix} \rho \\ \rho u \\ E \end{pmatrix} \quad \text{and} \quad F(W) = \begin{pmatrix} \rho u \\ \rho u^2 + p \\ u(E+p) \end{pmatrix}$$

where $E = \rho(\frac{1}{2}u^2 + \varepsilon)$. If $\varepsilon$ denotes the internal energy, then some law is required to close the whole system:

$$p = p(\rho, \varepsilon) \tag{9}$$

such that the Jacobian matrix may be diagonalized in $\mathbb{R}$ for $W \in \Omega$, $\Omega$ the set of admissible states, so that $\hat{\gamma}(p,\rho)p > 0$, $\rho > 0$, where:

$$\rho c^2(p,\rho) = \hat{\gamma}(p,\rho)p = \left(\frac{\partial \varepsilon}{\partial p}_{|\rho}\right)^{-1} \left(\frac{p}{\rho} - \rho \frac{\partial \varepsilon}{\partial \rho}_{|p}\right)$$

We also need to introduce entropy $s = s(p,\rho)$ which must comply with:

$$\hat{\gamma} p \frac{\partial s}{\partial p}_{|\rho} + \rho \frac{\partial s}{\partial \rho}_{|p} = 0 \tag{10}$$

Herein, $c$ stands for the speed of density waves.
The Jacobian matrix $A(W) = \dfrac{\partial F(W)}{\partial W}$ may be written:

$$A(W) = \begin{pmatrix} 0 & 1 & 0 \\ K - u^2 & u(2-k) & k \\ (K-H)u & H - ku^2 & u(1+k) \end{pmatrix}$$

setting $H = \frac{E+p}{\rho}$, $k = \frac{1}{\rho}\frac{\partial p}{\partial \varepsilon}_{|\rho}$, $K = c^2 + k(u^2 - H)$. Eigenvalues of the Jacobian matrix $A(W)$ read:

$$\lambda_1 = u - c,\ \lambda_2 = u,\ \lambda_3 = u + c$$

Recall that the 1-wave and the 3-wave are Genuinely Non Linear fields and that the 2-wave is Linearly Degenerated [20]. A sketch of the solution of the 1D Riemann problem is recalled below (see figure 5, which consists in four states labeled L, $1, 2$ and R separated by rarefaction waves, shocks and contact discontinuity, depending on the initial condition. In an alternative way, Euler equations may be written in a non conservative form, when restricting to smooth solutions.

## 4.2 Symmetrizing variables

Another way to rewrite Euler equations is to use symmetrizing variables:

$$Y(W) = {}^t(s, u, p)$$

defining matrices $B(Y)$ and $M(Y)$:

$$B(Y) = \begin{pmatrix} u & 0 & 0 \\ 0 & u\hat{\gamma}p\rho & \hat{\gamma}p \\ 0 & \hat{\gamma}p & u \end{pmatrix} \quad \text{and} \quad M(Y) = \begin{pmatrix} 1 & 0 & 0 \\ 0 & \hat{\gamma}p\rho & 0 \\ 0 & 0 & 1 \end{pmatrix}.$$

Obviously $B(Y)$ is symmetric and $M(Y)$ is symmetric positive definite, provided both density and pressure remain positive. Right eigenvectors of $(M)^{-1}(Y)B(Y)$ are:

$$r_1(Y) = \begin{pmatrix} 0 \\ \frac{1}{\rho} \\ -c \end{pmatrix}, \; r_2(Y) = \begin{pmatrix} 1 \\ 0 \\ 0 \end{pmatrix}, \; r_3(Y) = \begin{pmatrix} 0 \\ \frac{1}{\rho} \\ c \end{pmatrix}.$$

## 4.3 Approximate Godunov scheme VFRoe using symmetrizing variable

Turning now to the linearised problem, it may be easily checked that eigenvalues of $(M)^{-1}(\overline{Y})B(\overline{Y})$ are: $\tilde{\lambda}_1 = \overline{u} - \tilde{c}$, $\tilde{\lambda}_2 = \overline{u}$, $\tilde{\lambda}_3 = \overline{u} + \tilde{c}$, setting ; $\overline{\rho}(\tilde{c})^2 = \overline{\hat{\gamma}p}$. The decomposition of $Y_R - Y_L$ on the basis of right eigenvectors of $(M)^{-1}(\overline{Y})B(\overline{Y})$ provides intermediate states occuring in the linearised Riemann problem. While setting for any quantity $\psi$: $(\Delta\psi)_{LR} = \psi_R - \psi_L$, where subscripts $L, R$ refer to the left and right side of the initial discontinuity, coefficients $\tilde{\alpha}_1$ and $\tilde{\alpha}_3$ as introduced in the previous section are now:

$$\tilde{\alpha}_1 = \frac{1}{2\widetilde{\rho c}}(\overline{\rho}\widetilde{c}(\Delta u)_{LR} - (\Delta p)_{LR}) \quad \text{and} \quad \tilde{\alpha}_3 = \frac{1}{2\widetilde{\rho c}}(\overline{\rho}\widetilde{c}(\Delta u)_{LR} + (\Delta p)_{LR}).$$

The linearization has been made around the state ($\overline{\rho}$,$\overline{u}$,$\overline{p}$). Hence, the two intermediate states $Y_1, Y_2$ occuring in the solution of the *linearised* Riemann problem are the following:

$$Y_1 = \begin{pmatrix} s_L \\ u_L + \tilde{\alpha}_1 \frac{1}{\overline{\rho}} \\ p_L - \tilde{\alpha}_1 \widetilde{c} \end{pmatrix} \quad \text{and} \quad Y_2 = \begin{pmatrix} s_R \\ u_R - \tilde{\alpha}_3 \frac{1}{\overline{\rho}} \\ p_R - \tilde{\alpha}_3 \widetilde{c} \end{pmatrix}.$$

$$u_2 = u_1 = \overline{u} - \frac{1}{2\overline{\rho}\widetilde{c}}(\Delta p)_{LR} \tag{11}$$

$$p_2 = p_1 = \overline{p} - \frac{\overline{\rho}\widetilde{c}}{2}(\Delta u)_{LR} \tag{12}$$

Values $u_1 = u_2$ and $p_1 = p_2$ identify with intermediate values computed by any VFRoe scheme with variable $Y = {}^t(., u, p)$ (see [9] when focusing on $Y = {}^t(1/\rho, u, p)$). Intermediate values $s_1 = s_L$ and $s_2 = s_R$ are obviously physically releavant. The intermediate pressure (together with velocity and density) is set to its minimal value if $p_1$ is below the admissible range. This minimum is 0 for perfect gas EOS (or a mixture of perfect gases), or alternatively $-p_\infty$ for Tamman EOS ($\varepsilon = \frac{p+\gamma p_\infty}{(\gamma-1)\rho}$). This should not be confused with the standard clipping approximation which violates (with respect to time) the conservative form of discrete equations.

## 4.4 Some properties

*Property 2:* *a-* Intermediate value of pressure $p_1 = p_2$ remains positive provided that the initial conditions of the Riemann problem agree with condition:

$$(\Delta u)_{LR} < \frac{2\overline{p}}{\overline{\rho}\widetilde{c}} \tag{13}$$

*b-* Intermediate values of density $\rho_1$ and $\rho_2$ remain positive provided the latter condition is insured.

*Proof:* *a-* The proof is obvious since $p_1$ in (12) is positive if and only if (13) holds.
*b-* Intermediate states of density agree with:

$$\rho_1 = \rho(s_1, p_1) = \rho(s_L, p_1) \quad \text{and} \quad \rho_2 = \rho(s_2, p_2) = \rho(s_R, p_2)$$

Thus, the admissibility of $p_1 = p_2$ insures the admissibility of both $\rho_1$ and $\rho_2$.

This condition should be compared with the condition of existence and uniqueness of the solution of the Riemann problem for Euler equations with any EOS (and no vacuum occurence) which is [20],[5]:

$$(\Delta u)_{LR} < X_L + X_R \quad \text{where} \quad X_i = \int_0^{\rho_i} \frac{c(\rho, s_i)}{\rho} d\rho. \tag{14}$$

We here first restrict to perfect gas EOS ($p = (\gamma - 1)\rho\epsilon$, $1 < \gamma < 3$). Focusing on initial condition such that a double symmetrical rarefaction wave develops (that is : $Y_L =^t (s, u, p)$ and $Y_R =^t (s, -u, p)$ with $u < 0$), the condition (13) is more restrictive than its counterpart (14), unlike when dealing with shallow water equations. More precisely, numerical vacuum (in terms of pressure) occurs at the interface using VFRoe scheme as soon as $u/c > 1/\gamma$, whereas numerical vacuum (in terms of pressure or density) occurs at the interface with Roe scheme [3] as soon as $u^2/c^2 > 2/(\gamma(3-\gamma))$ and vacuum really arises when $u/c > 2/(\gamma - 1)$. Nonetheless, when plotting the ratio $p_{interface}/p$ as a function of $|u|/c$, it clearly appears that both curves associated with Godunov scheme and VFRoe scheme are monotone decreasing, whereas the one connected with Roe scheme is decreasing for $0 < |u|/c < 1/2$ and then increasing. Thus, though the constraint provided by Roe scheme to obtain releavant interface values of pressure and density is less restrictive than the one given by VFRoe scheme, the general behaviour of $p_{interface}/p$ vs $|u|/c$ is in better agreement with the exact Riemann solution [9] when applying VFRoe scheme. As a result, computations of safety valves with supersonic behaviour around the exit may blow up when using Roe scheme at the wall boundary instead of Godunov scheme (or VFRoe scheme), using the mirror technique in all cases. Anyway, even when condition (13) is fulfilled, there is no theoritical proof that cell values of pressure $p_i^n$ remain positive, when using the VFRoe scheme (or the Roe scheme). Nonetheless, appendix 7*b* shows the important fact that close to a wall boundary (where near-vacuum almost always appears in practice), the cell value of pressure will remain positive when a very strong rarefaction wave develops (that is to say when $U.n \leq 0$, where $n$ denotes the unit outward normal vector at the boundary), assuming standard CFL condition $CFL = 0.5$.

If we turn now to Tamman's EOS: $\varepsilon = \frac{p+\gamma p_\infty}{(\gamma-1)\rho}$ (and thus $s = (p + p_\infty)(\rho)^{-\gamma}$) , we emphasize that equation (12) may be read as $p_2 + p_\infty = p_1 + p_\infty = \overline{p + p_\infty} - \frac{\overline{\rho}\widetilde{c}}{2}(\Delta u)_{LR}$. Hence vacuum patterns (which turns to be $p + p_\infty = 0$ when focusing on this EOS) are similar than in the perfect gas framework. Results on discussion above thus hold true.

The scheme also benefits from the following properties, shared by all VFRoe schemes using variable $Y = {}^t(., u, p)$:

*Property 3:* Approximate values of intermediate states occuring in the linearized Riemann problem preserve invariance of $(u, p)$ variables through the numerical contact discontinuity.

The proof is trivial since inserting $u_L = u_R$ together with $p_L = p_R$ in equations $(11 - 12)$ results in: $u_1 = u_2 = u_L = u_R$ and also $p_1 = p_2 = p_L = p_R$.

*Property 4:* Assuming the state law takes the form:

$$\rho\varepsilon = f(p) + a\rho + b$$

where $a$ and $b$ are real constants, then cell values apart from a moving contact discontinuity preserve invariance of both velocity and pressure variables.

The proof may be found in appendix 8. Note that the latter family of internal energies includes not only perfect gas EOS, but also Tamman EOS and Tait EOS ($\varepsilon = \frac{p}{(\gamma-1)\rho} + A(\frac{1}{\rho} - \frac{1}{(\rho)_0})$). The reader is also referred to recent work by Saurel and Abgrall [21] for an alternative way to handle contact discontinuity when restricting to stiffened gas EOS, or to [22], [23] for more complex EOS.

## 4.5 Numerical results

A perfect gas state law has been used together with: $\gamma = \frac{7}{5}$. We first provide some results obtained using initial data in shock tube experiments, which generate vacuum. Hence, we use:

| | $\rho$ | $p$ | $u$ |
|---|---|---|---|
| Left | 1 | $10^5$ | $-4000$ |
| Right | 1 | $10^5$ | 4000 |

This results in a rather wide zone of vacuum. Actually, the limit Mach number in a symmetrical double rarefaction wave is $\frac{2}{\gamma-1}$ (which is thus equal to 5 here), whereas in the present case, the initial Mach number is approximately 11.7. The computational results were obtained using the following CFL number: $CFL = 0.45$, and a fine regular mesh with 12800 nodes (figures 6) respectively. Velocity profiles have been plotted though they are *meaningless* in the vacuum area. It must be emphasized that no clipping approximation is used here. Minimum values of density or pressure in the vacuum area are approximately $10^{-14}$ and $10^{-11}$ respectively.

The second series of results (figures 7) corresponds to the computation of a strong shock wave propagating over (near) vacuum. In this case, the initial data of the Riemann problem reads:

| | $\rho$ | $p$ | $u$ |
|---|---|---|---|
| Left | 1 | $10^5$ | 0 |
| Right | $1, 25.10^{-7}$ | $10^{-2}$ | 0 |

The sonic point in the 1-rarefaction wave requires introducing an entropy correction. The CFL number is the same as in previous cases. The mesh contains 3200 nodes here. These initial conditions typically result in a blow up of the code when using standard variable $Y = {}^t(\tau, u, p)$ (where $\tau = \frac{1}{\rho}$) as usually done [9] instead of the current symmetrizing variable.

The last series of results (figures 8) corresponds to the computation of a strong double shock wave, which shows again how the scheme behaves when computing impinging jets on wall boundaries. In this case, the initial data of the Riemann problem reads:

| | $\rho$ | $p$ | $u$ |
|---|---|---|---|
| Left | 1 | $10^5$ | 100 |
| Right | 1 | $10^5$ | $-100$ |

The regular mesh still contains 3200 nodes.

To conclude this part, we again provide below the true rate of convergence obtained when computing the standard Sod shock tube case, a double rarefaction wave and eventually a double shock wave, using first order (respectively second order) version of the scheme. We recall initial condition , which respectively are:

| | $\rho_L$ | $\rho_R$ | $p_L$ | $p_R$ | $u_L$ | $u_R$ |
|---|---|---|---|---|---|---|
| Sod shock tube | 1 | 0.125 | $10^5$ | $10^4$ | 0 | 0 |
| Double rarefaction wave | 1 | 1 | $10^5$ | $10^5$ | $-1200$ | 1200 |
| Double shock wave | 1 | 1 | $10^5$ | $10^5$ | 300 | $-300$ |

The second-order scheme is based on second-order Runge-Kutta time integration combined with standard MUSCL-type reconstruction of variables $\rho, u, p$ inside each cell. Plotting of $L^1$ error corresponds to density -squares-, velocity -triangles- and pressure -circles-. Straight lines correspond to the first-order scheme, and the dashed line refers to the second-order scheme. Results (see figures 9) are indeed very close to those provided in a previous work [9] when using variable $Y = {}^t(\tau, u, p)$, where $\tau = \frac{1}{\rho}$. An important point to emphasize is that the mean density converges slower than both pressure and velocity variables, unless the case is symmetric (figures 9 right top and bottom). This is due to the smearing of the contact discontinuity associated with eigen value $\lambda = u$, through which the density varies, whereas both pressure and velocity do not -or at least should not, since the latter are Riemann invariants through this wave-. The rate is close to 1 when restricting to $u, P$, when using the so-called second-order scheme, and is a bit lower for the density, especially when focusing on the Sod shock tube problem.

# 5 The K model

## 5.1 Governing equations

Governing equations of the convective part of the K model may only be written in non conservative form. These usually appear written in terms of the mean density $\rho$, the mean momentum $\rho u$, the mean total energy $E$ and the turbulent kinetic energy $K$ as follows, when focusing on perfect gas EOS:

$$\frac{\partial W}{\partial t} + \frac{\partial F(W)}{\partial x} + C(W)\frac{\partial W}{\partial x} = 0$$

setting:

$$W = \begin{pmatrix} \rho \\ \rho u \\ E \\ K \end{pmatrix} \quad \text{and} \quad F(W) = \begin{pmatrix} \rho u \\ \rho u^2 + p + 2\frac{K}{3} \\ u(E + p + 2\frac{K}{3}) \\ uK \end{pmatrix}$$

with $C(W)\frac{\partial W}{\partial x} = {}^t\left(0,0,0,2\frac{K}{3}\frac{\partial u}{\partial x}\right)$, and noting $E = \rho\frac{1}{2}u^2 + \rho\varepsilon + K$. Herein, $\varepsilon$ denotes the mean internal energy. The EOS for turbulent perfect gases is:

$$p = p(\rho, \varepsilon) = (\gamma - 1)\rho\varepsilon$$

The speed of mean density waves is modified by the presence of turbulence:

$$c^2(p, \rho, K) = \gamma\frac{p}{\rho} + 10\frac{K}{9\rho}$$

Introducing :

$$\mu = \frac{K}{(\rho)^{\frac{5}{3}}} \quad \text{and} \quad s = \frac{p}{(\rho)^{\gamma}}.$$

it is an easy matter to check that this system is a non strictly hyperbolic system. Real eigenvalues are:

$$\lambda_1 = u - c,\ \lambda_2 = \lambda_3 = u,\ \lambda_4 = u + c.$$

and associated right eigenvectors span $IR^4$. Both the 1-wave and the 4-wave are Genuinely Non Linear, whereas the 3-4-wave is Linearly Degenerated. Riemann invariants through the contact discontinuity are $\pi = p + 2K/3$ and $u$. Riemann invariants through the 1-wave are: $s = p\rho^{-\gamma}$, $\mu = K\rho^{-5/3}$,$u + Z$, and $s$, $\mu$,$u - Z$ through the 4-wave, while setting:

$$Z_i = \int_0^{\rho_i} \frac{c(\rho, s_i, \mu_i)}{\rho} d\rho$$

Moreover, assuming that the following jump conditions hold through shocks ($\sigma$ denotes the speed of the discontinuity separating states with subscripts $L$ and $R$):

$$\begin{gathered}
-\sigma[\rho]_{LR} + [\rho u]_{LR} = 0 \\
-\sigma[\rho u]_{LR} + [\rho u^2 + p + \tfrac{2K}{3}]_{LR} = 0 \\
-\sigma[E]_{LR} + [u(E + p + \tfrac{2K}{3})]_{LR} = 0 \\
-\sigma[K]_{LR} + [uK]_{LR} + \tfrac{2K_{LR}}{3}[u]_{LR} = 0
\end{gathered}$$

we recall [24] that the 1-dimensional Riemann problem associated with the latter problem and given initial data admits a unique solution with no vacuum occurence provided that the following condition holds:

$$u_R - u_L < Z_L + Z_R \tag{15}$$

## 5.2 Symmetrizing variables

Another way to write the latter equations is to use some symmetrisation variables. We focus here on $Y(W) = {}^t(u, \pi, \mu, s)$. Thus comes:

$$M(Y)\frac{\partial Y}{\partial t} + B(Y)\frac{\partial Y}{\partial x} = 0$$

with:

$$B(Y) = \begin{pmatrix} \rho^2 c^2 u & \rho c^2 & 0 & 0 \\ \rho c^2 & u & 0 & 0 \\ 0 & 0 & u & 0 \\ 0 & 0 & 0 & u \end{pmatrix} \quad \text{and} \quad M(Y) = \begin{pmatrix} \rho^2 c^2 & 0 & 0 & 0 \\ 0 & 1 & 0 & 0 \\ 0 & 0 & 1 & 0 \\ 0 & 0 & 0 & 1 \end{pmatrix},$$

$B(Y)$ is symmetric and $M(Y)$ is symmetric positive definite, provided that mean density, mean turbulent kinetic energy and mean pressure remain positive. Right eigenvectors of $(M)^{-1}(Y)B(Y)$ are:

$$r_1(Y) = \begin{pmatrix} \frac{1}{\rho} \\ -c \\ 0 \\ 0 \end{pmatrix}, \; r_2(Y) = \begin{pmatrix} 0 \\ 0 \\ 1 \\ 0 \end{pmatrix}, \; r_3(Y) = \begin{pmatrix} 0 \\ 0 \\ 0 \\ 1 \end{pmatrix}, \; r_4(Y) = \begin{pmatrix} \frac{1}{\rho} \\ c \\ 0 \\ 0 \end{pmatrix}.$$

### 5.3 Approximate Godunov scheme VFRoe using symmetrizing variable

We only provide here the main ingredients to construct the scheme.

$$\tilde{\alpha}_1 = \frac{1}{2\widetilde{c}}(\overline{\rho}\widetilde{c}(\Delta u)_{LR} - (\Delta\pi)_{LR}) \quad \text{and} \quad \tilde{\alpha}_4 = \frac{1}{2\widetilde{c}}(\overline{\rho}\widetilde{c}(\Delta u)_{LR} + (\Delta\pi)_{LR}).$$

The linearization is made around the state $(\overline{\rho}, \overline{u}, \overline{p}, \overline{K})$. Hence, the two intermediate states $Y_1, Y_2$ occuring in the solution of the *linearised* Riemann problem are the following:

$$Y_1 = \begin{pmatrix} u_L + \tilde{\alpha}_1 \frac{1}{\overline{\rho}} \\ \pi_L - \tilde{\alpha}_1 \widetilde{c} \\ \mu_L \\ s_L \end{pmatrix} \quad \text{and} \quad Y_2 = \begin{pmatrix} u_R - \tilde{\alpha}_4 \frac{1}{\overline{\rho}} \\ \pi_R - \tilde{\alpha}_4 \widetilde{c} \\ \mu_R \\ s_R \end{pmatrix}.$$

$$u_2 = u_1 = \overline{u} - \frac{1}{2\overline{\rho}\widetilde{c}}(\Delta\pi)_{LR} \tag{16}$$

$$\pi_2 = \pi_1 = \overline{\pi} - \frac{\overline{\rho}\widetilde{c}}{2}(\Delta u)_{LR} \tag{17}$$

### 5.4 Some properties

The Godunov scheme would naturally insure that $K_1, K_2, \rho_1, \rho_2$ and also $\pi_1 = \pi_2$ remain positive, assuming the scalar condition (15) holds true. Now we note that :

*Property 5: a-* Intermediate value of total pressure $\pi_1 = \pi_2$ remains positive provided that the initial conditions of the Riemann problem agree with:

$$(\Delta u)_{LR} < \frac{2\overline{\pi}}{\overline{\rho}\widetilde{c}} \tag{18}$$

*b-* Intermediate values of density $\rho_1$, $K_1$, $p_1$ and $\rho_2$, $K_2$, $p_2$ remain positive provided the latter condition is insured.

*Proof:* a- This clearly follows from equation (17).
b- Introducing $K_1 = \mu_L \rho_1^{5/3}$ and $p_1 = s_L \rho_1^{\gamma}$ in equation $\pi_1 > 0$ (due to condition (18)) enables to check that positive solution of $g(\rho_1) := \frac{2}{3}\mu_L \rho_1^{5/3} + s_L \rho_1^{\gamma} - \pi_1 = 0$ exists and is unique, since $g$ is a monotone increasing function from $[0, \infty]$ to $[-\pi_1, +\infty]$. Hence follows positivity of $K_1$, $p_1$. A similar result holds for $\rho_2$, $K_2$, $p_2$ on the other side of the contact discontinuity.

Once again, condition (18) is more restrictive than its continuous counterpart (15); this may be easily checked having a glance at the Riemann problem with a double symetric rarefaction wave. VFRoe scheme with $Y(W) = {}^t(u, \pi, \mu, s)$ also enables to preserve invariance of invariants $\pi$ and $u$ through the numerical contact discontinuity when computing the interface states.

*Property 6:* Assume that initial data in the Riemann problem agrees with:

$$u_R - u_L = 0$$
$$\pi_R - \pi_L = 0$$

Then intermediate states provided by VFRoencv scheme agree with the continuous condition since:

$$u_2 = u_1 = u_L = u_R$$
$$\pi_2 = \pi_1 = \pi_L = \pi_R$$

The proof is obvious owing to insertion of $\Delta u_{LR} = 0$ and $\Delta \pi_{LR} = 0$ in $(16 - 17)$. Now :

*Property 7:* Assuming the state law takes the form:

$$\rho\varepsilon = f(p) + a\rho + b$$

where $a$ and $b$ are real constants, then cell values apart from a moving contact discontinuity preserve invariance of both $u$ and $\pi$.

The proof is very similar to the proof of property 4 and thus is not detailed here. This means that the contact discontinuity is perfectly preserved when restricting to turbulent perfect gas EOS. *When focusing on turbulent real gas EOS, this property no longer holds.*

Though not discussed here, it is worth mentionning that use of other symetrizing variables such as $(U, P, K, s)$ does not enable to insure positive values of density, mean pressure and turbulent kinetic energy at the interface, unless one requires very hard constraints on initial conditions.

### 5.5 Numerical results

In figures 10 are plotted results on a mesh with 200 cells, setting $\gamma = 1, 4$, with the following initial conditions:

| | $\rho$ | $p$ | $u$ | $K$ |
|---|---|---|---|---|
| Left | 1 | $10^5$ | 0 | 100 |
| Right | 0.125 | $10^4$ | 0 | 1000 |

## 6 Conclusion

The use of symmetrizing variables thus allows computation of rather difficult flow configurations. It is emphasized that all schemes discussed herein rely on the Finite Volume techniques, and apply

for very simple approximate Riemann solvers at each interface between two neighbouring cells. The method has been successfully applied for shallow water equations, Euler equations, turbulent compressible closures based on one or two-equation models [24], [25] ( for second-order Reynolds stress closures, see reference[26]). The method has been proved to be as accurate as previous approximate Godunov schemes investigated [9], and meanwhile is more robust than similar approximate Godunov schemes in some specific cases including either real vacuum (when focusing on shallow water equations), or near-vacuum (when dealing with Euler equations for compressible gas dynamics). Measure of the $L^1$ error norm in some specific cases confirms that this solver is as accurate as Godunov scheme (shallow water equations) and of course much cheaper. Similar comments hold when turning to Euler equations. Though one might think that this kind of approach is much more in favour of the treatment of rarefaction waves, it nonetheless permits dealing with Riemann problems including strong double shock waves. The reason why the scheme converges towards the right weak solutions, despite from the fact that it uses so called non conservative variable, is due to the fact that it is written under conservative form.

These approximate Riemann solvers indeed seem promising to compute approximations of complex sets of equations such as those arising in two phase flow modelling [27], [21], [28],[29], [30]. In this frame, the counterpart of real vacuum may occur (when one phase disappears), as well as the near vacuum when strong rarefaction waves develop. These models indeed represent a hard challenge since they also involve many different time scales.

**Acknowledgments:**
The third author has benefitted from financial support under EDF-CNRS contract CO2770/AEE2704.

# References

[1] S.K. Godunov, A difference method for numerical calculation of discontinuous equations of hydrodynamics, *Mat. Sb.*, 1959, pp. 271–300. In Russian.

[2] E.F. Toro, *Riemann solvers and numerical methods for fluid dynamics*, Springer Verlag, 1997.

[3] B. Einfeldt, C.D. Munz, P.L. Roe and B. Sjögreen, On Godunov-type methods near low densities, *J. Comp. Phys.*, 1991, vol. 92-2, pp. 273–295.

[4] R.J. LeVeque, *Numerical Methods for Conservation Laws*, Birkhäuser-Verlag, Basel, 1990.

[5] E. Godlewski and P.A. Raviart, *Numerical approximation of hyperbolic systems of conservation laws*, Springer Verlag, 1996.

[6] P.L. Roe, Approximate Riemann solvers, parameter vectors and difference schemes, *J. Comp. Phys.*, 1981, vol. 43, pp. 357–372.

[7] G.A. Bird, *Molecular gas dynamics and the direct simulation of gas flows*, Clarendon, Oxford UK, 1994.

[8] E.S Oran, C.K. Oh and B.Z. Cybyk, Direct Simulation Monte-Carlo: recent advances and applications, *Ann. Rev. of Fluid Mech.*, 1998, vol. 30, pp. 403–441.

[9] T. Buffard, T. Gallouët and J.M. Hérard, A sequel to a rough Godunov scheme. Application to real gas flows, *Computers and Fluids*, 2000, vol. 29-7, pp. 813–847.

[10] T. Buffard, T. Gallouët and J.M. Hérard, A naive Godunov scheme to compute a non-conservative hyperbolic system, *Int. Series Num. Math.*, 1998, vol. 129, pp. 129–138.

[11] T. Gallouët, J.M. Hérard and N. Seguin, *Some recent Finite Volume schemes to compute Euler equations using real gas EOS*, LATP Report 00-021, Université de Provence, France. *to appear in Int. J. for Num. Meth. in Fluids*, 2000.

[12] A. Harten, P.D. Lax and B. Van Leer, On upstream differencing and Godunov-type schemes for hyperbolic conservation laws, *SIAM Review*, 1983, vol. 25, pp. 35–61.

[13] A. Harten, On the symmetric form of systems of conservation laws with entropy, *J. Comp. Phys.*, 1983, vol. 49, pp. 151–164.

[14] K. Jansen, Z. Johann and T.J.R. Hughes, Implementation of a one equation turbulence model within a stabilized finite element formulation of a symmetric advective-diffusive system, *Comput. Methods Appl. Mech. Engrg.*, 1993, vol. 105, pp. 405–433.

[15] J.M. Greenberg and A.Y. Le Roux, A well balanced scheme for the numerical processing of source terms in hyperbolic equation, *SIAM J. Numer. Anal.*, 1996, vol. 33-1, pp. 1–16.

[16] A.Y. Le Roux, Discrétisation des termes sources raides dans les problèmes hyperboliques, In *Systèmes hyperboliques : Nouveaux schémas et nouvelles applications*. Écoles CEA-EDF-INRIA "problèmes non linéaires appliqués", INRIA Rocquencourt (France), March 1998. Available on http://www-gm3.univ-mrs.fr/~leroux/publications/ay.le_roux.html, In French.

[17] T. Gallouët, J.M. Hérard and N. Seguin, *Some approximate Godunov schemes to compute shallow-water equations with topography*, EDF-DRD Report HI-81/01/05/A, *to appear in Computers and Fluids*, 2001.

[18] T. Gallouët and J.M. Masella, A rough Godunov scheme, *C. R. Acad. Sci. Paris*, 1996, vol. I-323, pp. 77–84.

[19] T. Buffard, T. Gallouët and J.M. Hérard, An approximate Godunov scheme to compute turbulent real gas flow models, *AIAA paper 99-3349*, 1999.

[20] J. Smoller, *Shock waves and reaction diffusion equations*, Springer Verlag, 1983.

[21] R. Saurel and R. Abgrall, A simple method for compressible multifluid flows, *SIAM J. Sci. Comp.*, 1999, vol. 21-3, pp. 1115–1145.

[22] K.M. Shyue, A fluid mixture type algorithm for compressible multicomponent flow with Van der Waals equation of state, *J. Comp. Phys.*, 1999, vol. 156, pp. 43–88.

[23] T. Gallouët, J.M. Hérard and N. Seguin, *An hybrid scheme to compute contact discontinuities in Euler systems*, EDF-DRD Report HI-81/01/011/A, *Submitted for publication*, 2001.

[24] A. Forestier, J.M. Hérard and X. Louis, A Godunov type solver to compute turbulent compressible flows, *C. R. Acad. Sci. Paris*, 1997, vol. I-324, pp. 919–926.

[25] J.M. Hérard, A. Forestier and X. Louis, *A non strictly hyperbolic system to describe compressible turbulence*, EDF-DER Report HE-41/94/011/A, 1994.

[26] C. Berthon, F. Coquel, J.M. Hérard and M. Uhlmann, An approximate solution of the Riemann problem for a realizable second moment turbulent closure, *Shock Waves*, 2002, vol. 11, pp. 245–269.

[27] T. Gallouët, J.M. Hérard and N. Seguin, An alternative way to deal with two fluid models, *AIAA paper 01-2653*, 2001.

[28] J. Glimm, D. Saltz and D.H. Sharp, Two phase flow modelling of a fluid mixing layer, *Journal of Fluid Mechanics*, 1999, vol. 378, pp. 119–143.

[29] V. Ransom and D.L. Hicks, Hyperbolic two-pressure models for two-phase flow, *J. Comp. Phys.*, 1984, vol. 53-1, pp. 124–151.

[30] M.R. Baer and J.W. Nunziato, A two phase mixture theory for the deflagration to detonation (DDT) transition in reactive granular materials, *Int. J. Multiphase Flow*, 1986, vol. 12-6, pp. 861–889.

# 7 Behaviour of cell values near wall boundaries

We introduce initial conditions of a Riemann problem which generate symmetrical double rarafaction waves, thus mimicking the exact behaviour of the approximate Godunov scheme, and wonder whether expected positive values (that is: water height (for shallow water equations); density and pressure (for Euler equations)) remain positive, *under classical CFL-like condition* :

$$CFL = V_{max}\lambda = 0.5 \tag{19}$$

while setting $\lambda = \frac{\Delta t}{h}$, and $V_{max}$ the maximum speed of waves.

## 7.1 Shallow water equations

We apply the classical mirror state technique, and assume that the initial condition in cell $w$ neighbouring the wall boundary is $(h_w^n = h, U_w^n = -U)$, and thus that mirror state in the fictitious cell on the right side of the wall boundary is :$(h_m^n = h, U_m^n = U)$, assuming that $U > 0$. Recall that vacuum occurs at the wall boundary if $2\sqrt{gh} = 2c \leq U$, otherwise not. Applying for the approximate Godunov scheme results in the following value $h_w^{n+1}$ at the end of the time step:

$$h_w^{n+1} - h + \lambda(hU) = 0$$

and thus $h_w^{n+1}$ identifies with prediction of Godunov scheme. Noting that CFL restriction necessarily implies that $\lambda U < 1$ insures that $h_w^{n+1}$ is positive.

## 7.2 Euler equations with perfect gas EOS

The EOS is assumed to be perfect gas EOS, hence : $P = (\gamma - 1)(E - 1/2\rho U^2)$, with $1 < \gamma < 3$. We still use the mirror state technique, and thus initial condition : $(\rho_w^n = \rho, U_w^n = -U, P_w^n = P)$ in the fluid cells on the left side of the wall, and $(\rho, U, P)$ in the mirror cell on the right side of the wall, assuming that $U > 0$. This may be in agreement with $(\gamma - 1)U < 2\sqrt{\gamma P/\rho}$ -in that case no vacuum occurs at the wall boundary-, or not. This initial data corresponds to the case called WBC in the main part of the paper, and also to the framework of analysis conducted in reference [3]. Setting $M = U/c$, and using the approximate Godunov scheme VFRoe with variable $Y^t = (s, U, P)$, the predicted value at the wall interface is simply :

$$s^* = s(\rho, P),\ U^* = 0,\ P^* = P(1 - \gamma M)$$

if $\gamma M < 1$, and otherwise:

$$s^* = s(\rho, P),\ U^* = 0,\ P^* = 0$$

Hence the updated cell value of density $\rho_w^{n+1}$ agrees with :

$$\rho_w^{n+1} - \rho + \lambda(\rho U) = 0$$

and thus still equals its counterpart obtained with the exact Godunov scheme. A similar result holds for total energy, since :

$$E_w^{n+1} - E + \lambda(U(E + P)) = 0$$

Nonetheless, predicted value of momentum on cell close to the wall

$$(\rho U)_w^{n+1} - (\rho U) + \lambda((\rho U^2) + P^* - P) = 0$$

differs from the one obtained with exact Godunov scheme, since values of pressure on the wall boundary are distinct : $P^* < P^*_{Godunov}$.
The above CFL-like condition may be rewritten as: $2\lambda c(1+M) = 1$.

*If* $0 < \gamma M < 1$, straightforward calculations show that :

$$\rho_w^{n+1} P_w^{n+1} = \frac{\rho P}{2(1+M)^2} g(M)$$

where :

$$g(M) = 8 + 4(3-\gamma)M + M^2(4 - 5\gamma + 3(\gamma)^2) + 2\gamma(\gamma-1)M^3$$

which is obviously positive when $M > 0$, since all four coefficients in the polynomial expression are positive when $1 < \gamma < 3$.

*If* $\gamma M > 1$, a similar result may be obtained, since :

$$\rho_w^{n+1} P_w^{n+1} = \rho P h(M)$$

where $h(M) = (1 - \frac{M - \sqrt{(\gamma-1)/(2\gamma)}}{2(1+M)})(1 - \frac{M + \sqrt{(\gamma-1)/(2\gamma)}}{2(1+M)})$ .

# 8 Numerical preservation of velocity and pressure through the contact discontinuity in Euler equations

We focus here on initial conditions of a Riemann problem, with uniform velocity and uniform pressure. Schemes investigated here can be derived from the formalism of VFRoe ncv scheme, with variable :

$$Y = {}^t(\varphi, u, p)$$

where $\varphi = \varphi(\rho, s)$ ($s$ denotes the specific entropy) must be independant of pressure $p$ (for instance $\varphi = s, \rho, \tau, ...$). Euler equations are rewritten in terms of $Y = {}^t(\varphi, u, p)$ as:

$$Y_{,t} + A(Y)Y_{,x} = 0$$

where :

$$A = \begin{pmatrix} u & \rho\varphi_{,\rho} & 0 \\ 0 & u & \rho^{-1} \\ 0 & \hat{\gamma}p & u \end{pmatrix}$$

The eigenvalues are ($c$ stands for the sound speed) :

$$\lambda_1 = u - c,\ \lambda_2 = u,\ \lambda_3 = u + c$$

and the associated right eigenvectors are :

$$r_1(Y) = \begin{pmatrix} -\frac{1}{c}\varphi_{,\rho} \\ \frac{1}{\rho} \\ -c \end{pmatrix},\ r_2(Y) = \begin{pmatrix} 1 \\ 0 \\ 0 \end{pmatrix},\ r_3(Y) = \begin{pmatrix} \frac{1}{c}\varphi_{,\rho} \\ \frac{1}{\rho} \\ c \end{pmatrix}$$

We recall that (see section 4.3) $Y_1$ and $Y_2$ read :

$$\begin{aligned} Y_1 &= Y_L + \widetilde{\alpha_1}\widetilde{r_1} \\ Y_2 &= Y_R - \widetilde{\alpha_3}\widetilde{r_3} \end{aligned}$$

where :

$$\begin{aligned} \widetilde{\alpha_1} &= -\frac{1}{2\tilde{c}}\Delta u + \frac{1}{2\tilde{\rho}\tilde{c}^2}\Delta p \\ \widetilde{\alpha_3} &= \frac{1}{2\tilde{c}}\Delta u + \frac{1}{2\tilde{\rho}\tilde{c}^2}\Delta p \end{aligned}$$

noting $\Delta(.) = (.)_R - (.)_L$. $Y_1$ and $Y_2$ do not depend on the choice of $\varphi$. Initial conditions generate an unsteady contact discontinuity:

$$\begin{aligned} \Delta u = \Delta p = 0 \quad &\Rightarrow \quad \widetilde{\alpha_1} = \widetilde{\alpha_3} = 0 \\ &\Rightarrow \quad Y_1 = Y_L \text{ and } Y_2 = Y_R \end{aligned}$$

These equalities are satisfied at each interface of the mesh. Hence, if we denote $\rho_{i+1/2}$ the numerical density of the linearised Riemann problem at the interface $i + 1/2$, $u_0$ and $p_0$ initial velocity and pressure, the Finite Volume scheme applied to the mass conservation equation gives :

$$\begin{aligned} \rho_i^{n+1} &= \rho_i^n - \frac{\Delta t}{\Delta x}((\rho u)_{i+1/2} - (\rho u)_{i-1/2}) \\ &= \rho_i^n - \frac{\Delta t}{\Delta x}u_0(\rho_{i+1/2} - \rho_{i-1/2}) \end{aligned}$$

Now, if we apply the Finite Volume scheme to the momentum conservation equation, we get :

$$\begin{aligned}
(\rho u)_i^{n+1} &= (\rho u)_i^n - \frac{\Delta t}{\Delta x}((\rho u^2 + p)_{i+1/2} - (\rho u^2 + p)_{i-1/2}) \\
&= (\rho u)_i^n - \frac{\Delta t}{\Delta x}((\rho_{i+1/2} u_0^2 + p_0) - (\rho_{i-1/2} u_0^2 + p_0)) \\
&= (\rho u)_i^n - \frac{\Delta t}{\Delta x} u_0^2 (\rho_{i+1/2} - \rho_{i-1/2}) \\
&= u_0 \left( \rho_i^n - \frac{\Delta t}{\Delta x} u_0 (\rho_{i+1/2} - \rho_{i-1/2}) \right) \\
&= u_0 \rho_i^{n+1}
\end{aligned}$$

Thus, $u_i^{n+1} = u_0$, $\forall i \in \mathbb{Z}$.
To study the discrete preservation of pressure, let us write the Finite Volume scheme applied to energy conservation equation :

$$\begin{aligned}
E_i^{n+1} &= E_i^n - \frac{\Delta t}{\Delta x}((u(E+p))_{i+1/2} - (u(E+p))_{i-1/2}) \\
&= E_i^n - \frac{\Delta t}{\Delta x} u_0 (E_{i+1/2} - E_{i-1/2})
\end{aligned}$$

Energy is defined by $E = \rho\varepsilon + \frac{1}{2}\rho u^2$. Thus:

$$(\rho\varepsilon)_i^{n+1} = (\rho\varepsilon)_i^n - \frac{\Delta t}{\Delta x} u_0 ((\rho\varepsilon)_{i+1/2} - (\rho\varepsilon)_{i-1/2})$$

Let us assume that the equation of state can be written under the form :

$$\rho\varepsilon = f(p) + b\rho + c \tag{20}$$

where $b$ and $c$ are real constants, and $f$ a inversible function (for instance perfect gas EOS, Tammann EOS, ...). If we introduce this equation of state in the previous equation, it gives :

$$\begin{aligned}
(f(p) + b\rho + c)_i^{n+1} &= (f(p) + b\rho + c)_i^n \\
&\quad - \frac{\Delta t}{\Delta x} u_0 ((f(p) + b\rho + c)_{i+1/2} - (f(p) + b\rho + c)_{i-1/2}) \\
f(p_i^{n+1}) + b\rho_i^{n+1} + c &= f(p_0) + b\rho_i^n + c \\
&\quad - \frac{\Delta t}{\Delta x} u_0 ((f(p_0) - f(p_0)) + b(\rho_{i+1/2} - \rho_{i-1/2}) + (c - c)) \\
f(p_i^{n+1}) &= f(p_0)
\end{aligned}$$

Thus, $p_i^{n+1} = p_0$.

Hence,provided that a state law can be written under the form (20), then a VFRoe ncv scheme, with variable $(\varphi, u, p)$, maintains uniform velocity and pressure profiles.

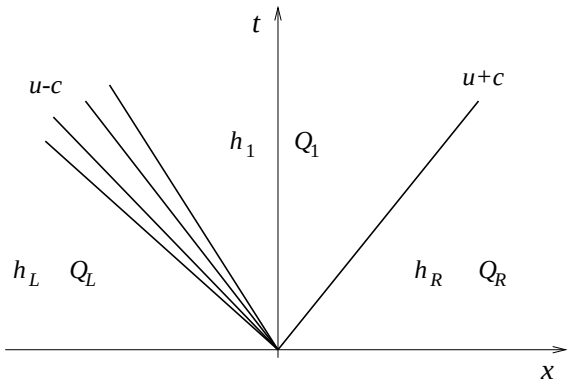


Figure 1: Solution of the 1D Riemann problem of SW equations

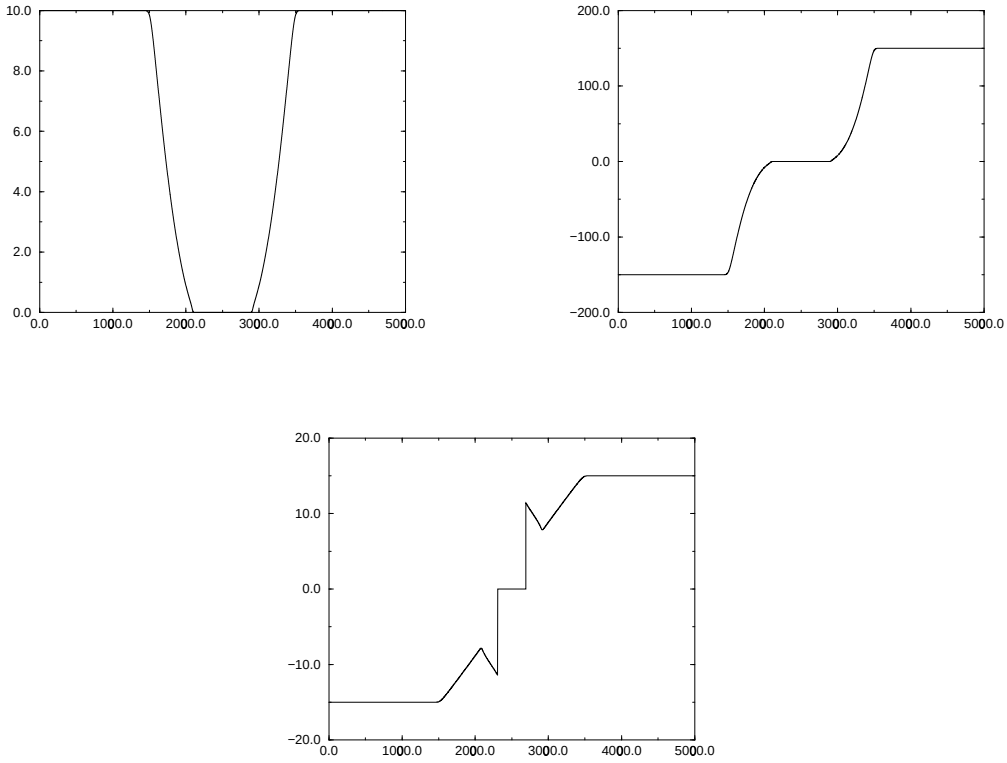


Figure 2: Dry area: water height (left top), momentum (right top), velocity (bottom), as functions of $x$

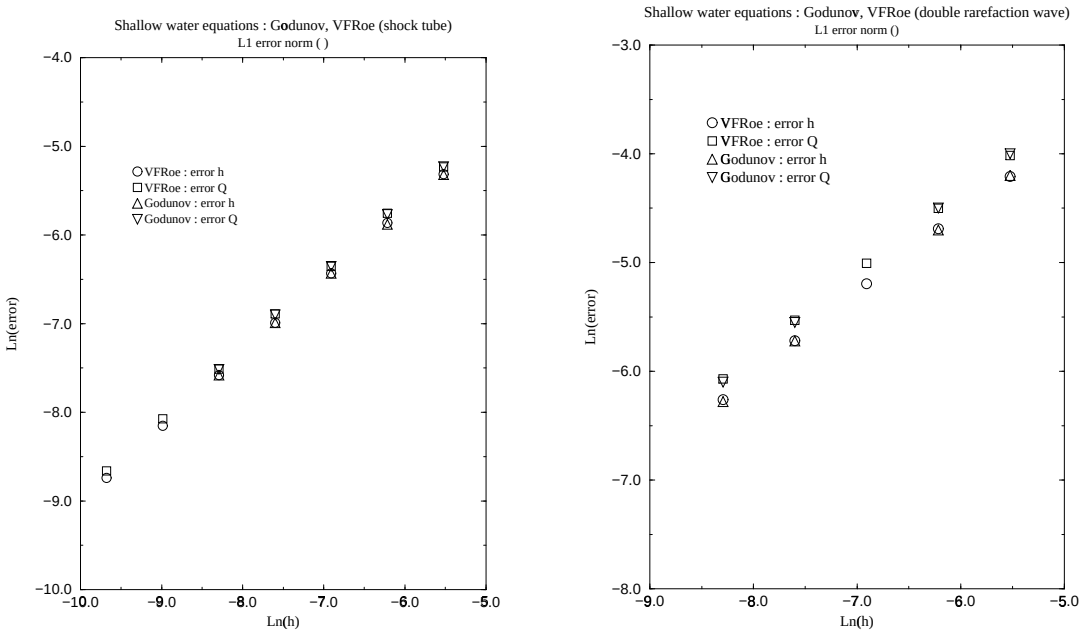


Figure 3: $L^1$ norm of the error

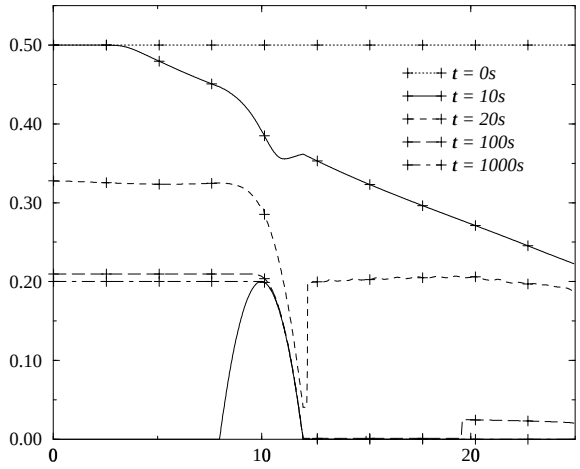


Figure 4: Dry area occuring when emptying a reservoir (water height as a function of x)

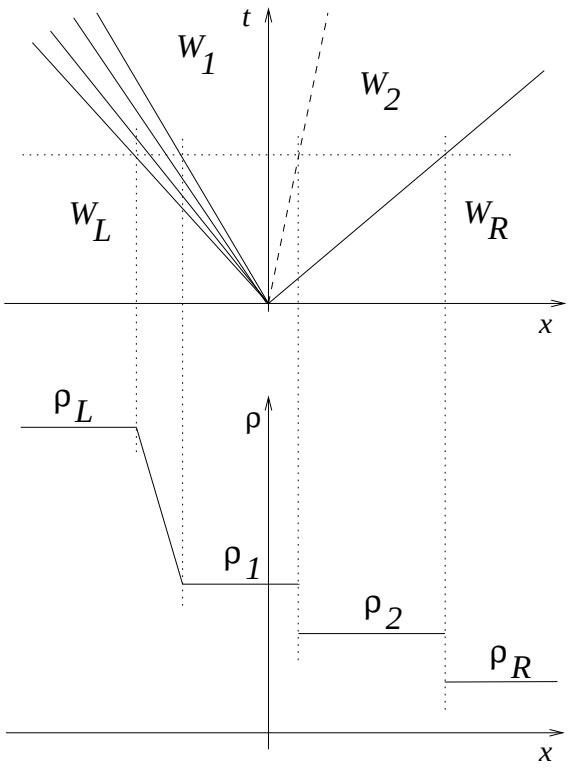


Figure 5: Solution of the 1D Riemann problem for Euler equations

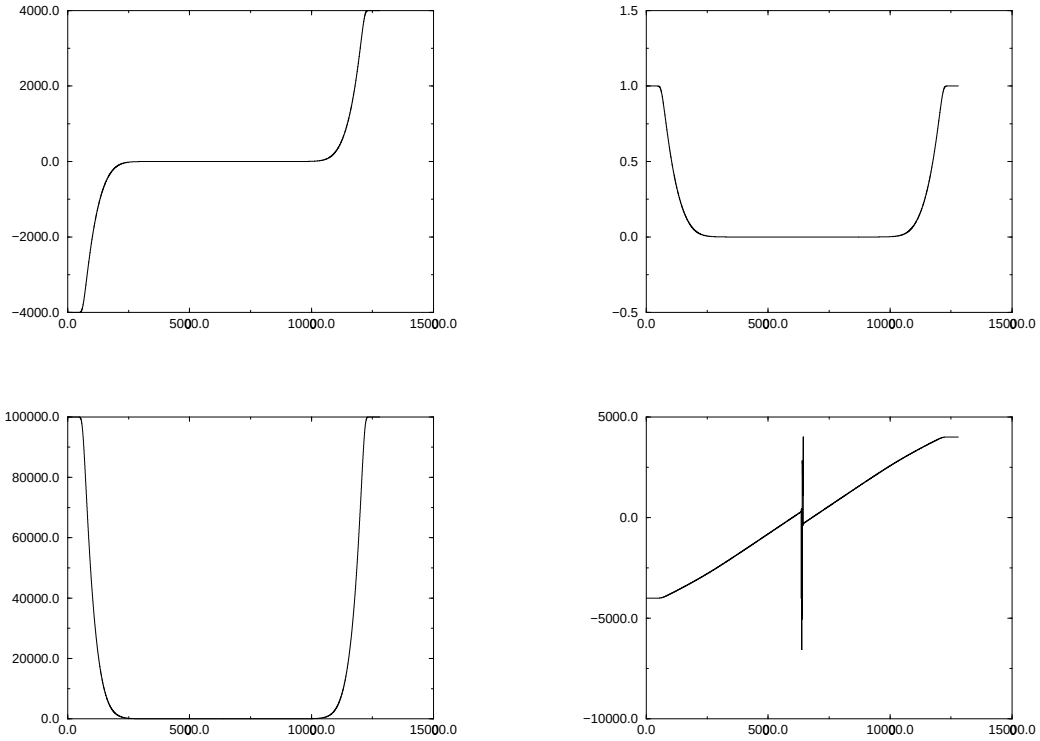


Figure 6: Vacuum occurence: momemtum (left top), density (right top), pressure (left bottom), velocity (right bottom), as functions of $x$

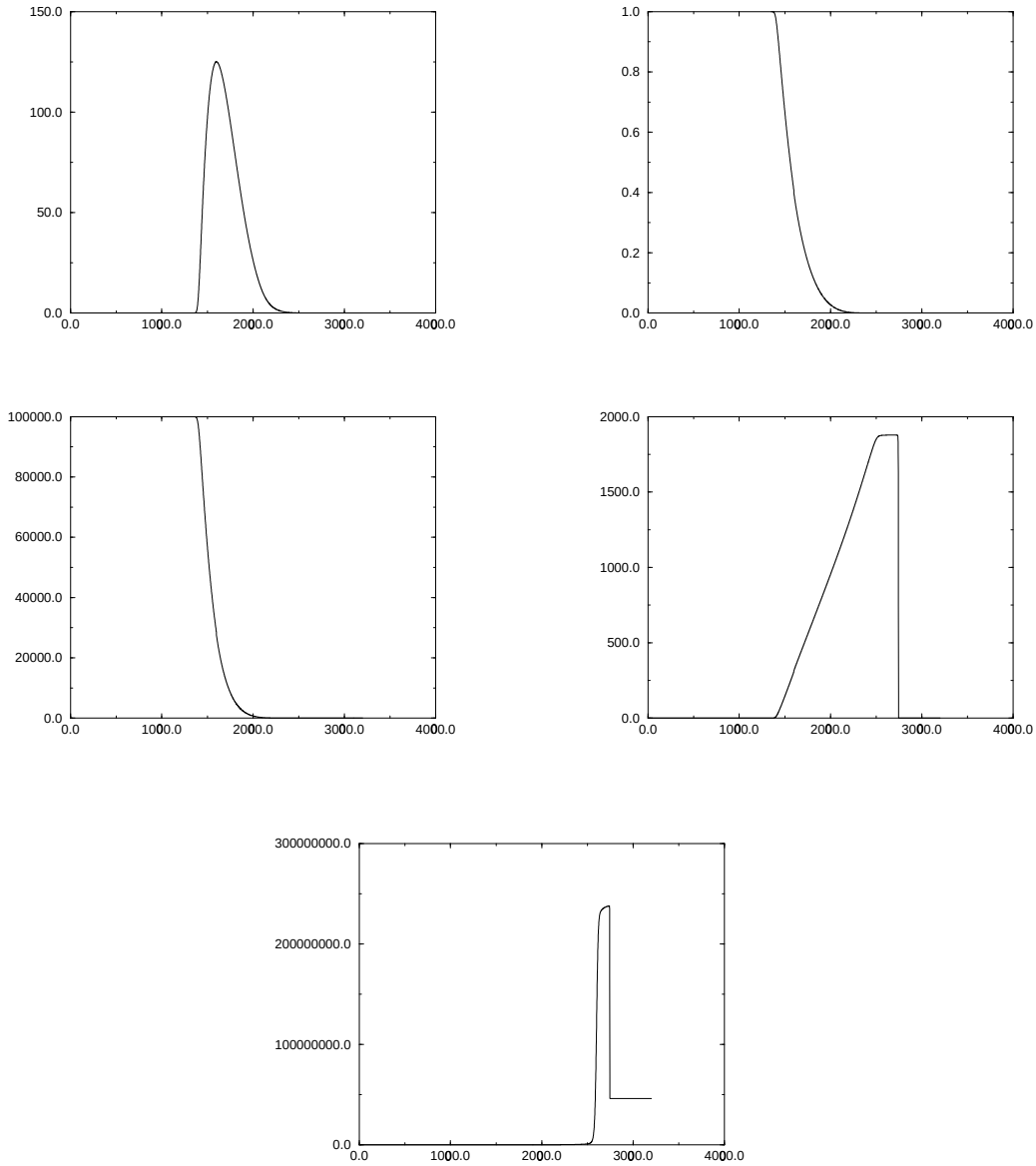


Figure 7: Shock wave over vacuum: momentum (left top), density (right top), pressure (left middle), velocity (right middle), specific entropy (bottom), as functions of $x$

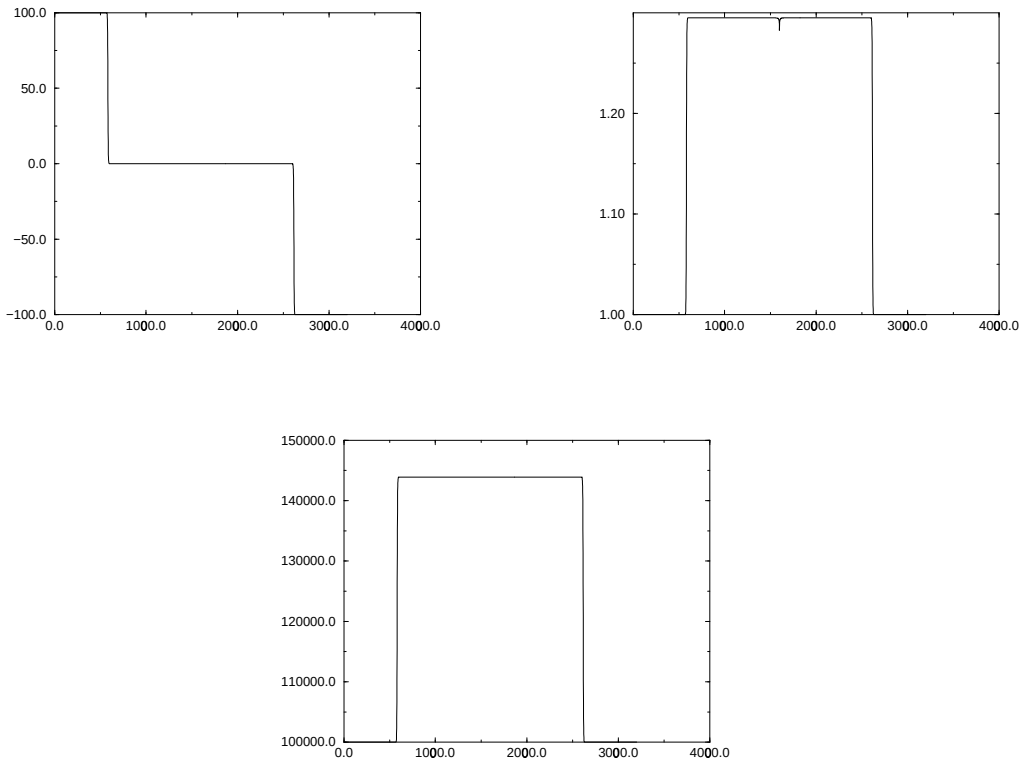


Figure 8: Double shock wave: momentum (left top), density (right top), pressure (bottom), as functions of $x$

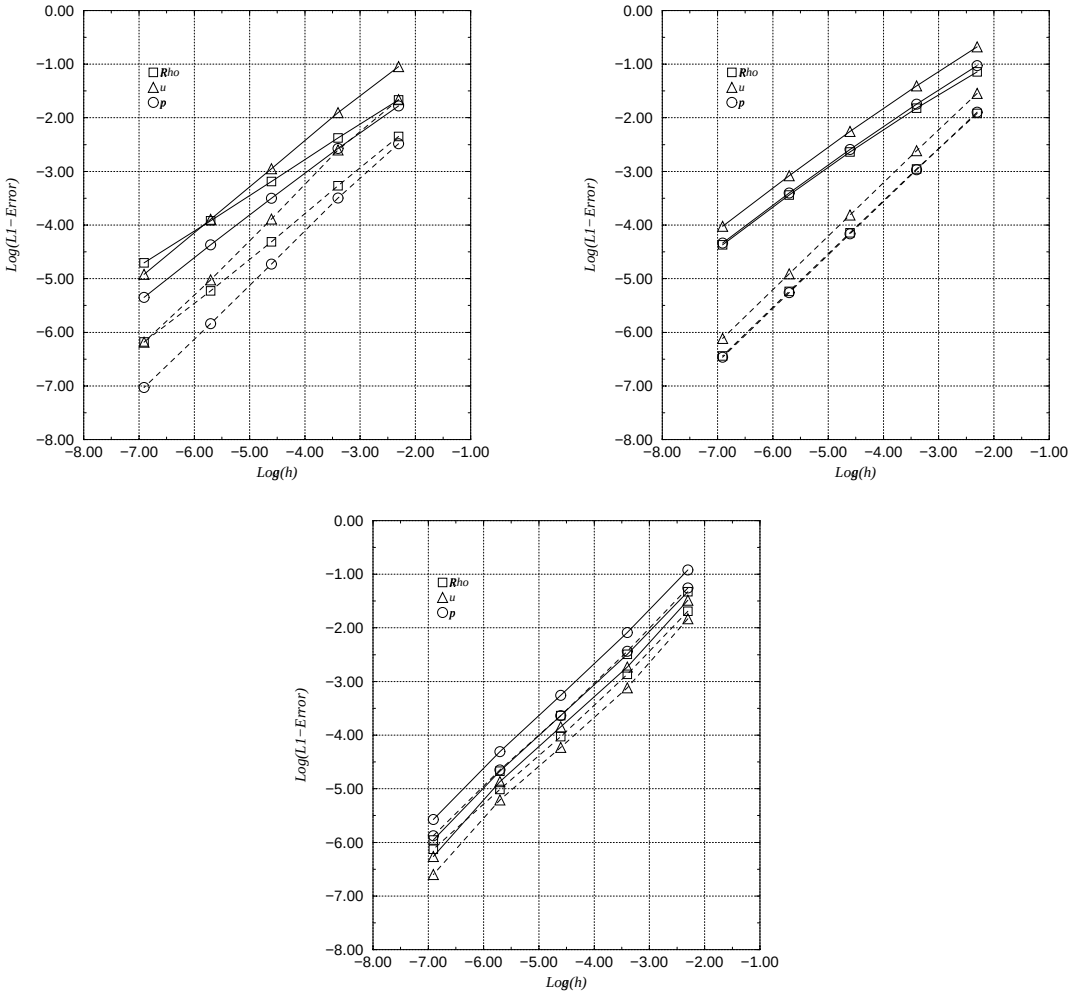


Figure 9: $L^1$ error norm - Sod shock tube (left top), double rarefaction wave (right top), double shock wave (bottom)

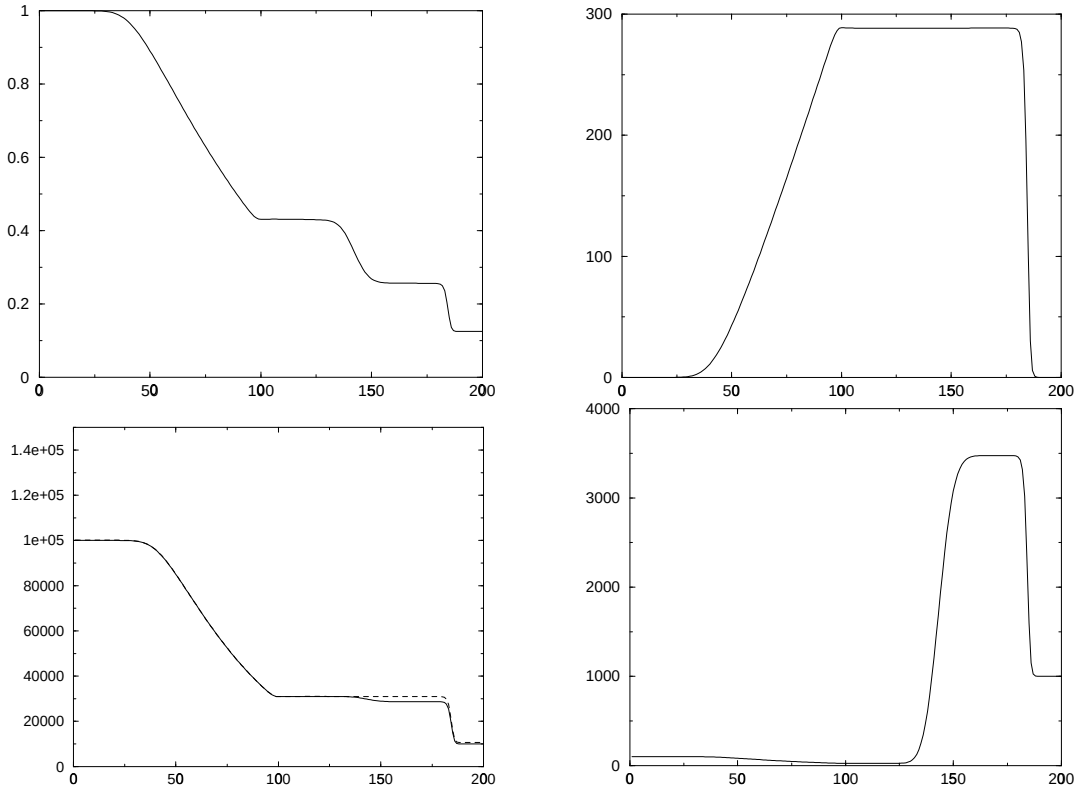


Figure 10: Turbulent Sod shock tube: density (left top), velocity (right top), $p$ (—) and $p + 2K/3$ (- -) (left bottom), $K$ (right bottom), as functions of $x$